

International Conference on Space Optics—ICSO 2004

Toulouse, France

30 March–2 April 2004

Edited by Josiane Costeraste and Errico Armandillo



SEVIRI, the imaging radiometer on Meteosat second generation: in-orbit results and first assessment

P. Coste, F. Pasternak, F. Faure, B. Jacquet, et al.



5th International Conference on Space Optics

SEVIRI, THE IMAGING RADIOMETER ON METEOSAT SECOND GENERATION: IN-ORBIT RESULTS AND FIRST ASSESSMENT

P. Coste, F. Pasternak and F. Faure ^a, B. Jacquet and S. Bianchi ^b, Donny M. A. Aminou, H. J. Luhmann ^c,
C. Hanson, P. Pili, G. Fowler ^d

^a EADS ASTRIUM, 31, Rue des Cosmonautes, 31402 Toulouse Cedex 4, France
E-mail: Pierre.Coste@astrium.eads.net

^b ALCATEL Space Industries, 100 Boulevard du Midi, 06150 Cannes La Bocca, France

^c ESA/ESTEC Keplerlaan 1, P.O. Box 299, 2200 AG Noordwijk, The Netherlands

^d EUMETSAT, Am Kavalleriesand 31, 64295 Darmstadt, Germany

ABSTRACT

Meteosat Second Generation (MSG) is a series of 3 geo-stationary satellites developed and procured by the European Space Agency (ESA) on behalf of the European Organisation for the Exploitation of Meteorological Satellites (EUMETSAT). The first satellite (MSG-1) was launched on August 29, 2002 by an Ariane 5 rocket.

SEVIRI is the main MSG payload and produces 12 channels imaging in visible and IR range. The 8 Infrared Channels in the 3.9-13.4 mm band benefit from high radiometric performances thanks to the use of detectors operating at 95K and cooled by specifically designed passive radiator. During the commissioning phase, dedicated tests have been conducted to verify the SEVIRI functionality and performances. This paper presents briefly the SEVIRI design and highlights the correlation of data obtained in-flight by EUMETSAT with the ground predictions.

A particular emphasis is put on the in-orbit evolution of the IR channel gains and on the instrument decontamination.

1. PRESENTATION OF SEVIRI

1.1. HISTORY

The Spinning Enhanced Visible and InfraRed Imager (SEVIRI) is the new generation of geo-stationary orbit imaging instrument for Meteorological application. It succeeds the Meteosat Radiometers that are in orbit since 1977. SEVIRI studies started at the end of the 80's as inputs to the Meteosat Second Generation program. The development phase started in 1994. SEVIRI is a completely new instrument compared to the

Meteosat Radiometer, with 12 spectral channels, faster imaging and improved performances.

The MSG satellite has been manufactured by a consortium led by ALCATEL SPACE, under ESA responsibility. The satellite and ground segment is owned and operated by EUMETSAT. The satellite commissioning is under EUMETSAT responsibility and performed by EUMETSAT with the support of ESA and industry. EADS ASTRIUM is the prime contractor for the SEVIRI instrument.

The first flight model was delivered in 1999 after less than 5 years of development and extensive testing and integrated in the MSG1 satellite, launched on Ariane 513 on August 29, 2002.

The commissioning of the MSG-1 satellite and SEVIRI instrument has been conducted up to January 2004. More than one year of testing and data acquisition has provided a lot of information showing excellent performances.

1.2. SEVIRI IMAGING PRINCIPLE

The imaging mission corresponds to a continuous image taking of the Earth in the 12 spectral channels with a baseline repeat cycle of 15 minutes.

The East/West earth scanning is realized by the satellite spin at 100 rpm. Image lines are acquired at rates over 7.5 Msamples/sec, and "slowly" transferred during the remaining of the 0.6 s revolution.

The South/North scanning is realized by a Scan Assembly. This accurate mechanism supporting a 500 x 800 mm light-weighted mirror is designed for a 7-year lifetime, meaning 245 000 cycles.

The total 15 minutes repeat cycle is reached after internal IR calibration, scan retrace and stabilisation.

Large image size allows for high spatial resolution from geo-stationary orbit:

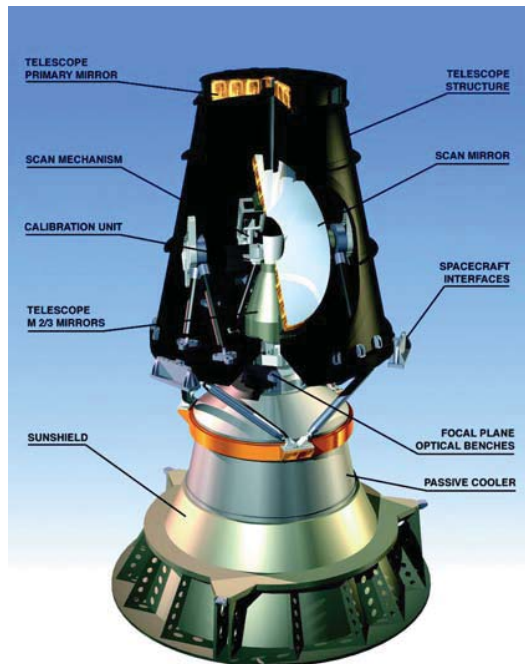
- 5625 x 11250 pixels for the 1 km sampling channel (HRV)
- 3750 x 3750 pixels for the other 3 km channels

This demanding optical system is achieved through a patented 3-mirror telescope concept providing the capability of in-orbit calibration using an accurate calibration reference source inserted in the optical path by the Calibration Unit.

1.3. SEVIRI OVERVIEW

The Instrument is split into 4 main subassemblies :

- Telescope and Scan Assembly (TSA)
- Focal Plane and Cooler Assembly (FPCA)
- Sunshield
- Electronic Units: Preamplifier Unit (PU), Main Detection Unit (MDU) and Functional Control Unit (FCU)



TSA and FPCA are coupled to form the SEVIRI Main Unit

1.4. SPECTRAL CHANNELS

SEVIRI provides 12 spectral channels acquired simultaneously and geometrically co-registered. Each channel is named by its central wavelength in microns.

Channel	Comments
HRV	Broadband high resolution channel
VIS0.6	Cloud mapping
VIS0.8	Vegetation index
NIR1.6	Cloud / snow discrimination
IR3.9	Atmospheric window
IR6.2	Water vapour channel
IR7.3	Water vapour channel
IR8.7	Atmospheric window
IR9.7	Ozone channel
IR10.8	Atmospheric window
IR12.0	Atmospheric window
IR13.4	Carbon dioxide channel

SEVIRI spectral channels

1.5. TELESCOPE AND SCAN ASSEMBLY

The Telescope and Scan Assembly (TSA) includes the telescope optics, the telescope structure and the mechanism assemblies. The 5367 mm focal length telescope is based on a three-mirror concept.

The telescope structure relies on the use of a central stiff base plate, which interfaces with the spacecraft via three isostatic mounts, a CFRP cone, providing the aperture to the spacecraft baffle and supporting the Primary Mirror M1. The FPCA is attached to the TSA by mean of a 6 titanium strut arrangement.

The TSA includes the three SEVIRI mechanisms :

- The Scan Assembly operates the Image North/South scanning
- The Refocusing Mechanism (REM) allows for focus adjustments
- The CALU allows the precise in-orbit calibration of the infrared channels by insertion of the small Calibration Reference Source (CRS) into the optical beam

1.6. THE FOCAL PLANE AND COOLER ASSEMBLY (FPCA)

The Passive Cooler Assembly (PCA) is a two-stage passive cooling device, composed of the Radiator and the Sunshield, which provide the infrared detectors with a cryogenic environment.

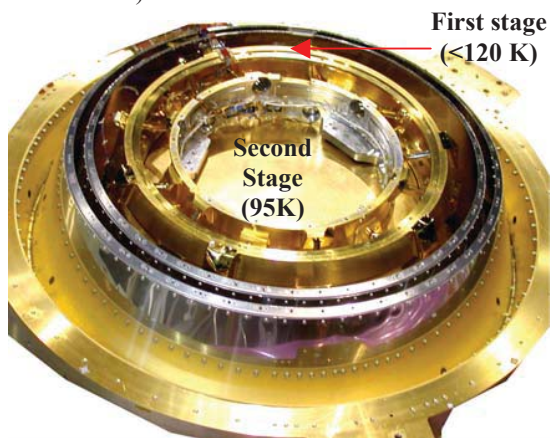
The Sunshield avoids direct solar fluxes on the first and second stages of the Radiator. In addition, the sunshield radiation on the second-stage is minimised by design of the internal cone elliptical shape.



SEVIRI Instrument Main Unit during integration, showing the TSA cone aperture

The PCA is equipped with heaters, in order to allow for periodic decontamination of the instrument.

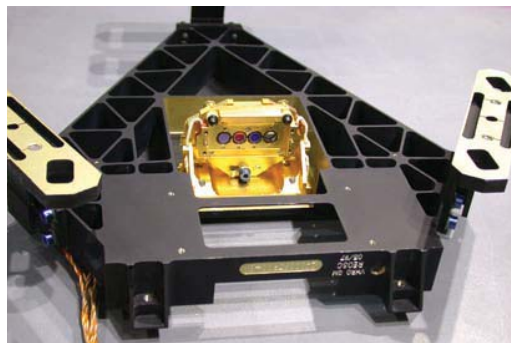
The Detection Cold Wiring (DCW) that provides the electrical connection between the detectors located in the cold part (CIRO) and the warm part of the instrument is submitted to a thermal gradient of about 200 K. The DCW has been optimised in order to comply with the electrical requirements whilst minimizing the thermal losses. Structurally, the CIRO is thermally de-coupled from the warm part by a set of low-conductive suspensions (12 GFRP struts) and a dedicated GFRP cone.



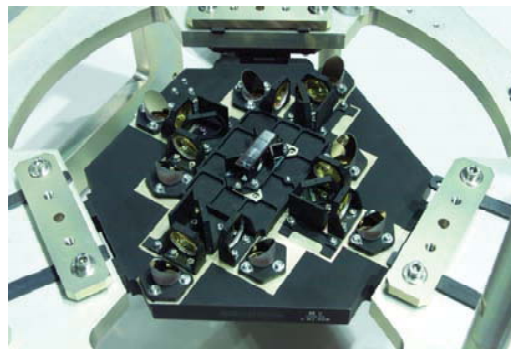
Radiator Internal view without the Optical benches: first and second stages are thermally isolated through “suspensions”

The FPOB consist of three main assemblies shown in the figures below.

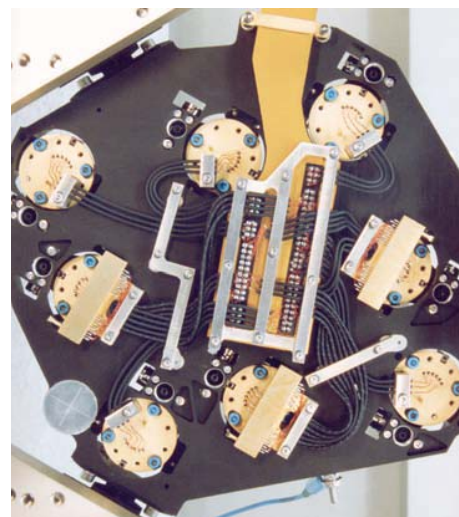
The IR detectors are all in cadmium-mercury telluride (CMT), whereas the visible detectors are in silicium (Si) and the NIR detector is in indium-gallium arsenide (InGAs).



VNIR and HRV Optical Bench (VHRO) holds the 4 visible channels detector package and filters regulated at 20°C



Warm IR Optical Bench (WIRO) provides in-field beam separation at the telescope focal plane level and splits the 8 IR channels



Cold IR Optical Bench (CIRO), thermally regulated at 85 K or 95 K, holds the 8 IR Detector packages. Three IR-PV channels require proximity electronic, the Cold Units (CU) hybrids.

2. IN-ORBIT THERMAL BEHAVIOUR

2.1. INTRODUCTION

The SEVIRI telemetries presented in this paper cover more than eight months from the first switch ON of the instrument end of November 2002 up to August 2003. The temperature evolutions over the whole period are shown and commented in the figures below. An interruption of the telemetries can be seen on all the curves during a few days beginning of April 2003 corresponding to a temporary switch OFF of the instrument.

All telemetry data used in this presentation are reproduced by courtesy of EUMETSAT.

2.2. THERMAL BEHAVIOUR

By design, the SEVIRI instrument is strongly thermally decoupled from the spacecraft so that the main driver of the instrument in-orbit temperature is the sun elevation angle as illustrated in the Fig. 1 below.

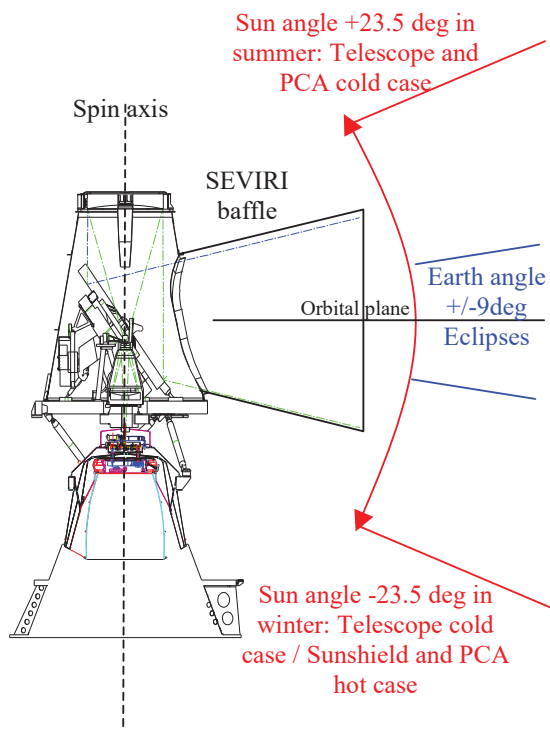


Fig. 1: Sun angle evolution with respect to SEVIRI

2.2.1. TEMPERATURE TELEMETRIES

As shown and detailed below, the in-orbit thermal behaviour and temperatures of the instrument are consistent with the predictions, with differences corresponding to nominal design margins taking

into account worst-case environment and spacecraft interfaces and end-of-life conditions. The transients in eclipse and the instrument gradients are very well correlated with the predictions.

The Fig. 2 represents the temperatures of different telescope parts (structure baseplate and cone, scan and primary mirrors).

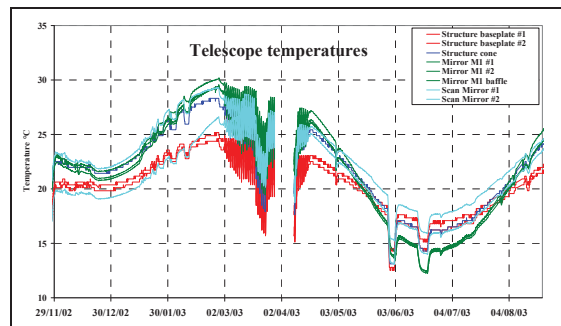


Fig. 2: Telescope temperatures over whole observation period

The telescope temperatures present a 6 months period. The minimal values, around 15°C, occur during the summer solstice period when the solar flux input within the telescope cavity is minimum. On the opposite, the maximal values, between 25 and 30°C, occur just before the eclipse period when the solar flux is close to the maximum and not interrupted by eclipses. This in-orbit behaviour is fully consistent with the SEVIRI thermal analysis which predicted the maximum 22 days before the equinox.

The oscillations on the curves in March and beginning of April correspond to the eclipses, during which the telescope temperatures drop by a few degrees. Other variations seen in the curves (e.g. mid-June) correspond to transient spacecraft or instrument operations not discussed in this paper.

The Fig. 3 below shows the telescope temperatures over three consecutive days around the maximum eclipse period. The eclipse effect, leading to a temperature decrease by 2 to 5°C, appears clearly and is in line with the predictions.

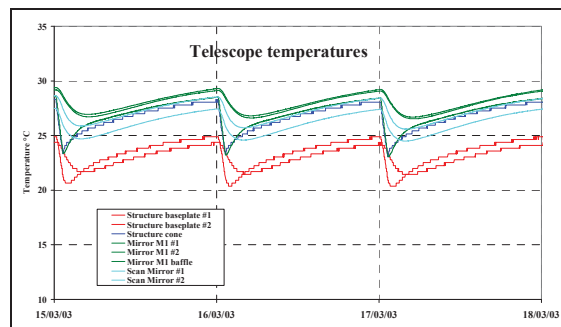


Fig. 3: Telescope temperatures over 3 days in eclipse period

The Fig. 4 shows the evolution of the sunshield temperature.

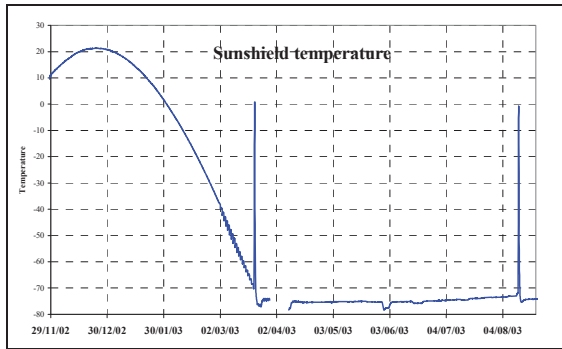


Fig. 4: Sunshield temperature

The temperature increases up to 22°C around the winter solstice when the solar angle is minimum and then the flux in the sunshield maximum. When the sun angle is above 0°C after the spring equinox, there is no more solar input and the sunshield temperature remains nearly constant around its lowest value of -75°C. Small oscillations due to the eclipses can also be seen in March. The two spikes up to 0°C in March and August correspond to the two sunshield decontaminations which followed the Passive Cooler ones (see §2.3).

The Fig. 5 represents the temperature of the first stage of the Passive cooler. Its evolution follows the sunshield temperature, which drives the amount of emitted flux entering the cooler. The maximum temperature is about 125 K whereas the minimum operating temperature is about 107 K. The spikes in March and August correspond to the two cooler decontaminations (see §2.3).

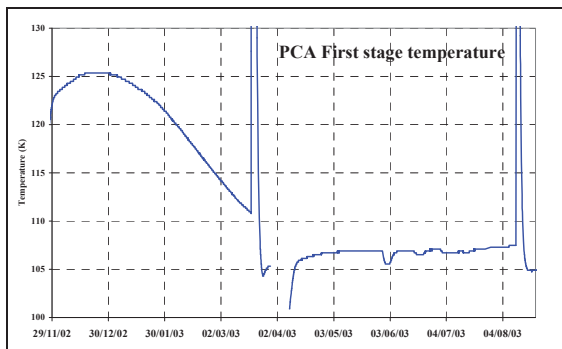


Fig. 5: PCA First stage temperature

2.2.2. PCA SECOND STAGE THERMAL REGULATION

The regulated Passive cooler second stage temperature is shown Fig 6, together with the corresponding thermal control current.

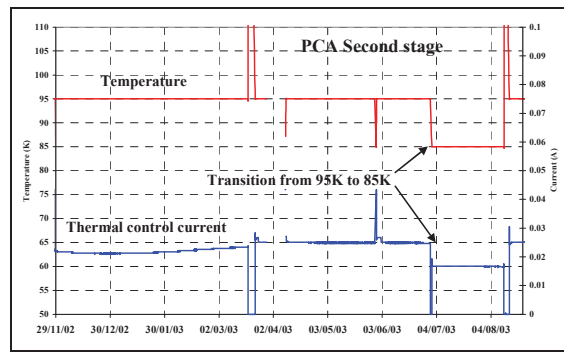


Fig. 6: PCA Second stage regulation

The two nominal operating temperatures of the PCA second stage are 95K and 85K. SEVIRI on ground performance and characterisation tests have been done at these two temperatures. The value of 95 K is the predicted nominal hot case, providing regulation margins even in worst PCA thermal conditions. The regulation at 85K may be used in PCA cold case in order to improve the radiometric performances of the IR channels, in particular for the long wavelengths (IR10.8, IR12.0 and IR13.4). The current in-orbit results show that the operating temperature could in fact be continuously maintained at 85 K.

The transition from 95 K to 85 K beginning of July corresponds to a drop of the regulation current from 25 mA to 16.7 mA, consistent with the predictions (see Fig. 7).

The evolution of the regulation current depends mainly on the cooler thermal environment driven by the sunshield temperature. The minimum regulation need (i.e. lowest current) corresponds to the maximum temperature of the sunshield and PCA first stage. The effect of the March decontamination is also noticeable. The increase of the regulation current after the decontamination reflects the improvement of the cooler efficiency. This is described in more details in §2.3. The effect of the second decontamination in August is less obvious since the regulation temperature is not the same before and after the decontamination, so that direct comparison is not possible.

The Fig. 7 below compares the measured regulation power in orbit with the predictions in the PCA cold case (summer), showing a very good consistency between both.

Regulation power	In orbit	Prediction
At 95 K	≈ 340 mW	320 mW
At 85 K	≈ 150 mW	150 mW

Fig. 7: Comparison of 2nd stage thermal regulation need with predictions

2.2.3. PCA NON-OPERATING CASE

The first instrument switch ON in November and the switch ON in April after about 10 days switched OFF provided PCA non operating temperature measurements summarised in Fig. 8 below.

	First switch ON in November	Switch ON in April
First stage temperature	120 K	101 K
Second stage temperature	74 K	64 K (*)

Fig. 8: PCA non operating temperatures

(*) The 64 K measurement is out of the nominal calibrated range of the PCA second stage thermistance and is therefore not accurate. The analysis show that the actual temperature was at least 2 K more, i.e. above 66 K. In any case, this 2nd stage temperature measurement is consistent with the coldest predicted temperature of 65 K, showing both the prediction accuracy and the high performance of the SEVIRI Passive Cooler.

The Fig. 9 illustrates the April switch ON of the thermal regulation, showing again the excellent behaviour of the 2nd stage thermal control loop with the very rapid convergence when it reaches 95K.

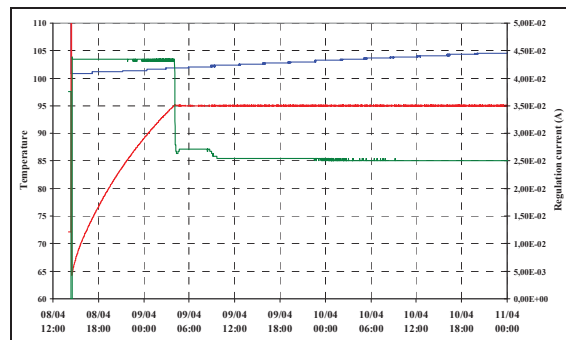


Fig. 9: PCA temperatures at switch ON

2.3. DECONTAMINATION

The SEVIRI provides the capability to heat up the Passive Cooler in order to decontaminate the second stage and therefore the cold part of the IR channel optical path from accumulated frozen contaminants. The sunshield can also be heated for decontamination.

Three decontaminations have been done up to the end of 2003: the first one (24 h duration) after launch to remove as much contaminants as possible before the first radiator cool down, the second one in March (48 h duration) and the third one in August (24 h duration). In each case, a 8-hour sunshield decontamination followed the Passive Cooler one. Another decontamination has been

done in January 2004 before the start of the operational phase.

The Fig. 10 illustrates the March decontamination. The chronological sequence of events is described below.

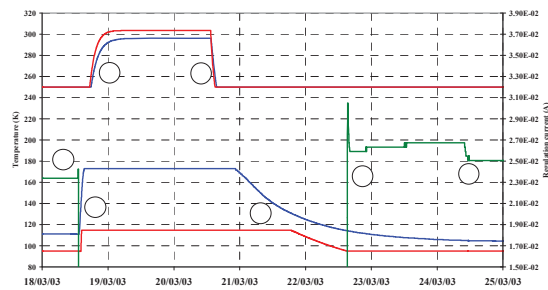


Fig. 10: PCA March decontamination

1. Before starting the heating, the 2nd stage (red) is regulated at 95K. The regulation current (green) is 23.4 mA. The first stage temperature (blue) is 111 K. The dedicated decontamination thermistances (above curves) are saturated.
2. The 1st and 2nd stage heating starts. The 1st stage heaters are switched ON about 45 minutes before the 2nd stage ones following the foreseen scenario optimised with respect to the constraints in the 2nd stage suspensions. The 2nd stage thermistance reaches its saturation limit within a few minutes and the 1st stage one in less than 2 hours.
3. Within a few hours, the temperatures enter the range of the decontamination thermistances. The temperature stabilisation is reached after about 18 hours. The heating power is such that the second stage temperature (30°C) is above the first stage one (23°C) to optimise the decontamination efficiency. These temperatures are well in line with the predictions.
4. The heating is stopped after 48 hours. The temperatures drop quickly out of the decontamination thermistance range.
5. After a duration ranging from about 10 hours for the first stage and 30 hours for the second stage, the temperatures enter again in the nominal thermistance ranges.
6. After about 2 days of cooling, the second stage reaches 95 K and the thermal regulation is switched ON. The temperature stabilises very quickly. The regulation current still increases afterwards, following the first stage cool down which is slower than the second stage one due to its much higher thermal inertia.
7. The detection chains are switched ON. The power dissipated by the IR detectors and proximity electronics leads to a rapid decrease of the required regulation current. The observed current drop corresponds to about 45mW strictly in line with the expectation.

The difference between the regulation current after and before the sequence reflects the improvement of the cooler efficiency due to the decontamination. The main effect is however the spectacular improvement of the IR detection chain gains as shown in §2.4.

The Fig. 11 illustrates the August decontamination. The chronological sequence of events is similar to the March one. The main differences are:

- The starting 2nd stage temperature is 85 K whereas it is 95 K after the decontamination. As a consequence, the starting regulation current is also lower (see Fig. 7) and cannot be directly compared to the current at the end.
- The decontamination duration is 24 h instead of 48 h. This is however sufficient to reach the temperature stabilisation.
- The IR chains are already ON at re-start of the regulation (step 6). The regulation current drop associated to the detection chain switch ON visible in step 7 of the March decontamination is therefore not present here. The slow increase of the current following the 1st stage stabilisation is however still visible here.

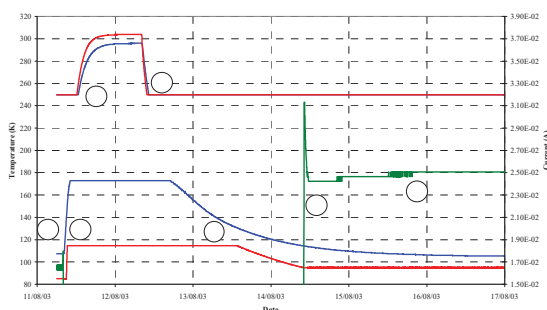


Fig. 11: PCA August decontamination

2.4. IR CALIBRATIONS AND GAIN EVOLUTIONS

As described in chapter 1, the SEVIRI instrument provides a Calibration Unit (CALU) for the in-orbit calibration of the IR channels. The CALU is designed to be used once per image (15-minute period). It moves the Calibration Reference Source (CRS) at the intermediate telescope focal plane. The CRS temperature is monitored by a high accuracy thermistance.

The complete calibration of the IR chain gains requires three measurements: one of the background level, obtained during deep space viewing at each satellite rotation, and two of the CRS at 15 minutes interval and at two different temperatures. For the first measurement, the CRS is

floating at ambient telescope temperature. For the second one, it is heated between 15°C and 20°C above the ambient temperature. This concept allows a high accuracy gain calibration as proven by the on ground analyses and tests.

The first in-orbit calibration was done on December 2nd 2002 a few days after the first instrument switch ON. This first calibration showed significant lower gains - between 5% and 40% depending on the IR channel - with respect to the ground measurements done first at EADS ASTRIUM level during the instrument acceptance tests and later confirmed at satellite level.

These gain drops, homogenous between the different chains of a same channel, were attributed to contamination, accumulated during the first three months in orbit. The most affected channels were the long wavelength ones: IR12.0, IR13.4 and IR10.8.

The numerous calibrations done during the following months showed a further regular decrease of the gains also consistent with a progressive accumulation of contaminants in the PCA second stage.

In March, a 48-hour decontamination of the Passive Cooler was performed as described in §2.3. The calibrations done afterwards, end of March and in April showed a spectacular increase of the IR chain gains, which all nearly recovered, or even slightly exceeded, the level measured during the SEVIRI ground tests.

These results confirmed that the gain drop was actually due to contamination and, above all, they clearly demonstrated the decontamination efficiency.

These results are illustrated in Fig. 12 showing the IR gain evolution from the first calibration in orbit up to November 2003.

The 100% references in the figures correspond to the values measured on ground during the performance tests in vacuum at EADS ASTRIUM level. These ground test results are shown in the figures as the values at launch.

The figures show clearly the steps after the two decontaminations, in particular after the March one. Only one chain per channel is shown for clarity but the results are similar for the 3 chains of the same channel. The gains in July and August during the period of 2nd stage regulation at 85 K are not included since the IR chains, in particular the IR-C ones, have significantly different (better) values than at 95 K.

The data after both decontaminations show again a decrease of the gains but at a significantly smaller rate than before. This means that contaminants are still present. This is also in line with the prediction from the contamination analysis done during the design phase of the instrument. Contamination is indeed expected to occur during the whole in-orbit life but with a decreasing rate. Regular decontaminations are foreseen to maintain optimal IR channel performances.

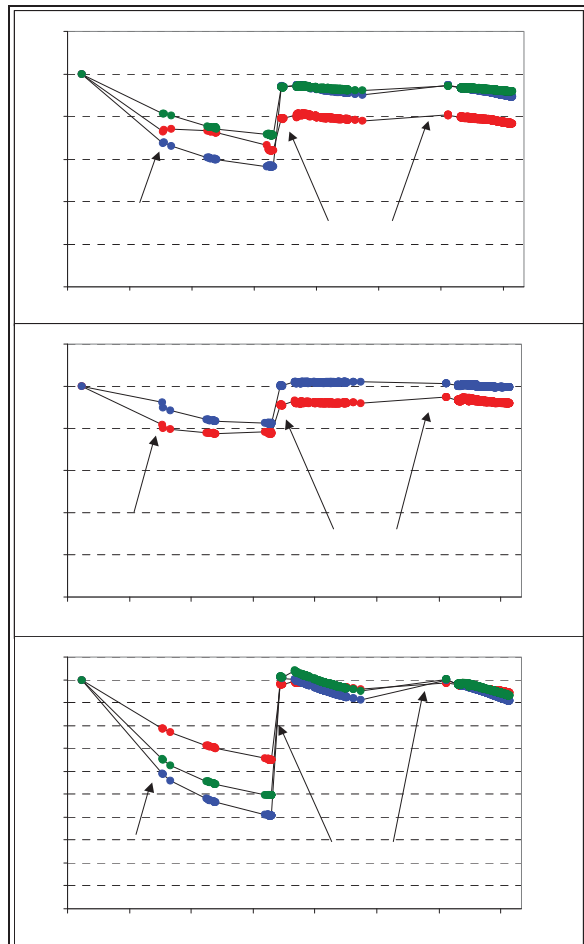


Figure 3/12: IR gain evolution from first calibrations in orbit up to Nov 2003 normalised to ground measurements

3. CONCLUSION

This paper presented an overview of the SEVIRI design and the first results relative to both the instrument thermal behaviour and the gain evolution in orbit, including the spectacular effect of the decontamination.

These results demonstrate a good correlation with predictions, in particular in several areas for which

the Radiator design had been optimised and which obviously could not be fully tested on ground : the sun illumination effect, the evolution of the contamination on the cold parts and the decontamination procedure efficiency.

As a general statement, the performance results achieved in orbit during the commissioning show that MSG-1 raw images are of excellent quality providing significant margins with respect to the specification. A presentation of the radiometric and imaging performances is given in ⁽²⁾.

The SEVIRI Flight Models 2 and 3 are already manufactured and have shown similar performances to the first model during their ground tests. A fourth model production has been started in 2003.

4. ACKNOWLEDGEMENTS

The authors wish to thank all people at EUMETSAT, ESA, ALCATEL SPACE and EADS ASTRIUM who contributed to this paper.

In particular, the Authors wish to thanks the EUMETSAT people who provided the in-flight data for this article.

EADS ASTRIUM also wishes to thank the whole SEVIRI Industrial team for the high involvement of each subcontractor in the Instrument development.

5. REFERENCES

- (1) Meteosat Second Generation: The Satellite Development, European Space Agency, BR-153, November 1999
- (2) Meteosat Second Generation In-Flight Commissioning of the Imaging radiometer SEVIRI, SPIE Conference Remote Sensing 2003 San Diego, D. M. A Aminou* and A. Ottenbacher, European Space Agency, B. Jacquet, S. Bianchi, Alcatel Space Industries, P. Coste, Astrium SAS
- (3) EUMETSAT Technical Note reference EUM/MSG/RPT/465, «MSG-1 Decontamination Test», COM n° 523 200, issue 2 dated 02 July 2003
- (4) EUMETSAT web site (www.eumetsat.de), in particular MSG1 Commissioning and Images sections